Catalysis of methyl viologen radical reactions by polymer-stabilized gold sols

ARTICLE *in* THE JOURNAL OF PHYSICAL CHEMISTRY · JANUARY 1981

Impact Factor: 2.78 · DOI: 10.1021/j150602a015

Catalysis of Methyl Viologen Radical Reactions by Polymer-Stabilized Gold Sols[1]

D. Meisel,* W. A. Mulac, and M. S. Matheson

Chemistry Division, Argonne National Laboratory, Argonne, Illinois 60439 *(Received: April 30, 1980; In Final Form: September 15, 1980)*

The catalysis of methyl viologen radical cation ($MV^{+}\cdot$) decay reactions by gold sol, stabilized by either poly(vinyl sulfate) (PVS) or poly(vinyl alcohol) (PVA), was studied by pulse radiolysis. Stabilization of the sol by PVS eliminates the hydrogen evolution reaction as a pathway for $MV^{+}\cdot$ decay. This is shown to be due to dimerization of $MV^{+}\cdot$ (to the biradical) in the potential field of the polyelectrolyte. On PVA-stabilized sols, the hydrogen evolution reaction is a major pathway although side reactions (probably hydrogenation) interfere to a large extent. The rate of adsorption of $MV^{+}\cdot$ on PVA-stabilized sol is controlled by the diffusion of $MV^{+}\cdot$ to the gold particle. Subsequent reactions of protonation and electrochemical desorption, $(Au)_c^{n}H_m + H_3O^{+} \rightarrow (Au)_c^{(n-1)}H_{m-1} + H_2 + H_2O$, on a slower time scale are the rate-determining steps at the pH range and catalyst concentration used. At higher catalyst concentrations interparticle reaction is invoked to explain the dependence on [Au].

Introduction

Hydrogen production from water by reactive intermediates has been shown to proceed efficiently in the presence of redox catalysts. Many recent reports, now available in the literature, have substantiated the notion that such redox catalysts, and in particular metallic colloids, can make the hydrogen evolution reaction[2-10] compete favorably with the other modes of reaction that such intermediates usually will undergo. A wide variety of reductants, produced photochemically, thermally, or radiolytically, as well as several metallic catalysts, have been shown to operate in these systems. Among the most frequently used sources of reducing equivalents for this purpose is the methyl viologen radical cation ($MV^{+}\cdot$). The ease of reduction of MV^{2+}, the exceptionally long lifetime of the radical, and its strong absorption in the visible spectral range make the $MV^{+}\cdot$ radical a particularly convenient candidate for such studies. In the present report, we study the kinetics and mechanistic behavior of the hydrogen evolution reaction of $MV^{+}\cdot$ on polymer-stabilized gold sols.

Although the participation of metallic colloids in the catalysis of hydrogen production from water is now well documented, the details of the various steps involved in this catalysis are still unclear. In a recent report[11] a direct observation of $MV^{+}\cdot$ decay catalyzed by colloidal Pt was shown to occur in the submillisecond time scale. Such a fast decay was attributed to a diffusion-controlled reaction of the radical with the metal particles. A detailed mechanistic model for the catalysis of the hydrogen evolution reaction on silver colloids was recently suggested by Henglein.[9] In this mechanism, much like the common mechanism for the electrochemical hydrogen evolution reaction, the metallic particle is charged by the reducing radical. Following this charging reaction protonation occurs and finally H_2 desorption. Since the gold sols have recently been shown to operate through basically the same mechanism,[12] the present results will be discussed in terms of this mechanism. Problems relevant to the particular metal and the stabilizers used will be outlined.

Experimental Section

Materials. Two types of gold sols, both prepared by reduction of $HAuCl_4$ by CO, were used in this study. The procedure for the preparation of the poly(vinyl sulfate) (PVS) gold sol has been described previously.[12] The other sol was stabilized by poly(vinyl alcohol) (PVA, Polysciences, Inc., 133 000 molecular weight). Approximately 100 mg of $HAuCl_4$ was dissolved in 500 mL of 0.1% PVA, and the pH adjusted with NaOH to ~11. CO gas was then bubbled through the solution for 10 min at room temperature. The resultant sol was then acidified with $HClO_4$ to pH 2.5 and then boiled for 1 h to expel CO or CO_2. The sol thus obtained had a spectrum similar to that of the Au/PVS sol previously described.[12] Both sols were found to obey Beer's law in the range of concentrations described in this study. Unless otherwise stated, concentrations for Au are given in terms of Au atoms and for the polymer stabilizers in terms of monomer units. Both sols were stable for many weeks without any noticeable deterioration in their absorption spectra. Nonetheless, sols for irradiations were freshly prepared. All other materials were of highest purity commercially available and were used as received. Triply distilled water was used throughout this study.

Procedure and Instrumentation. Solutions were deaerated or saturated with the desired gas by using the syringe technique. Unless otherwise stated, all solutions used in this study contain 1% v/v 2-propanol and 1% v/v acetone.

For steady-state irradiations a ^{60}Co γ source was used at dose rates of 0.72–8.1 krd/min. Gaseous products of the irradiaton were measured on a Van-Slyke manometer directly connected to a gas chromatograph (Infotronics 153C, dual 13X molecular sieve columns, Ar carrier). A

(1) This work was performed under the auspices of the Office of Basic Energy Sciences of the U.S. Department of Energy.

(2) Koryakin, B. V.; Dzhabiev, T. S.; Shilov, A. E. *Dokl. Akad. Nauk. SSSR* **1977**, *233*, 359.

(3) (a) Lehn, J. M.; Sauvage, J. P. *Nouv. J. Chim.* **1977**, *1*, 449. (b) Kirch, M.; Lehn, J. M.; Sauvage, J. P. *Helv. Chim. Acta* **1979**, *62*, 1345.

(4) Moradpour, A.; Amouyal, E.; Keller, P.; Kagan, H. *Nouv. J. Chim.* **1978**, *2*, 547.

(5) Okura, I.; Kim-Thuan, N. *J. Mol. Catal.* **1979**, *5*, 311.

(6) (a) Kalyanasundaram, K.; Kiwi, J.; Grätzel, M. *Helv. Chim. Acta* **1978**, *61*, 2720. (b) Kiwi, J.; Grätzel, M. *Angew. Chem., Int. Ed. Engl.* **1979**, *18*, 624.

(7) Kawai, T.; Tanimura, K.; Sakata, T. *Chem. Lett.* **1979**, 137.

(8) DeLaive, P.; Sullivan, B. P.; Meyer, T. J.; Whitten, D. G. *J. Am. Chem. Soc.* **1979**, *101*, 4007.

(9) (a) Henglein, A. *J. Phys. Chem.* **1979**, *83*, 2209. (b) Ibid. **1979**, *83*, 2858.

(10) (a) Krasna, A. *Photochem. Photobiol.* **1979**, *29*, 267. (b) Ibid. **1980**, *31*, 75.

(11) Kiwi, J.; Grätzel, M. *J. Am. Chem. Soc.* **1979**, *101*, 7214.

(12) Kopple, K.; Meyerstein, D.; Meisel, D. *J. Phys. Chem.* **1980**, *84*, 870.

0022-3654/81/2085-0179$01.00/0

few experiments on the isotopic composition of $H_2/HD/D_2$ in H_2/D_2 saturated sols were performed on a CEC 21-620 mass spectrometer. The pulse radiolysis–spectrophotometric detection system has been previously described.[13a] Transient spectra were recorded by using the streak camera technique.[13a,b] Some experiments were performed by using the pulse radiolysis–conductivity system as previously described.[13c] Pulse widths of 2–40 ns, producing 5–60 μM total concentration of radicals per pulse, were used in this study. Data analysis was done on a Sigma V computer.

Results and Discussion

Formation of $MV^{+\cdot}$ in the Presence of the Catalysts. The radical cation in the presently studied systems was generated by the sequence of reactions 1–5. The total

$$H_2O \rightsquigarrow e_{aq}^-, \dot{O}H, H\cdot, H_2, H_2O_2, H^+ \quad (1)$$

$$e_{aq}^- + (CH_3)_2CO \xrightarrow{H^+} (CH_3)_2\dot{C}OH \quad (2)$$

$$(CH_3)_2CHOH + \dot{O}H \rightarrow (CH_3)_2\dot{C}OH + H_2O \quad (3)$$

$$(CH_3)_2CHOH + H\cdot \rightarrow (CH_3)_2\dot{C}OH + H_2 \quad (4)$$

$$(CH_3)_2\dot{C}OH + MV^{2+} \rightarrow MV^{+\cdot} + (CH_3)_2CO + H^+ \quad (5)$$

yield of $MV^{+\cdot}$ is therefore expected to be $G(MV^{+\cdot}) = G_{e_{aq}^-} + G_{OH} + G_H = 6.2$ molecules/100 eV. (This value may however be slightly overestimated since some OH radicals will probably yield β-hydroxy radicals. On the other hand, the G values used above should be somewhat increased because of spur scavenging reactions at the high scavenger concentration used.) In the absence of acetone, reaction 2 is replaced by direct reduction of MV^{2+} by e_{aq}^- (reaction 6). Under the latter conditions $MV^{+\cdot}$ is formed in two

$$e_{aq}^- + MV^{2+} \rightarrow MV^{+\cdot} \quad (6)$$

well-separated steps, a faster process attributed to reaction 6 ($k_6 = 8.4 \times 10^{10}$ M^{-1} s^{-1}) and a slower process (reaction 5). From the rate of the formation of the absorption at 605 nm, we obtain for the slower process $k_5 = (3.5 \pm 0.2) \times 10^9$ M^{-1} s^{-1}. From the absorbance observed at the end of this reaction and taking $G(MV^{+\cdot}) = 6.2$, we get $\epsilon_{605} = 1.19 \times 10^4$ M^{-1} cm^{-1}. Similar values were obtained by various methods for preparation of $MV^{+\cdot}$. The ratio of the absorbance observed at the end of the reaction 5 to that observed at the end of reaction 6 (in the absence of acetone) yields a value of 2.3, in close agreement with $(G_{e_{aq}^-} + G_{OH} + G_H)/G_{e_{aq}^-} = 2.2$. The spectral features at the end of reaction 5 are in agreement with the well-documented spectrum of $MV^{+\cdot}$, and we therefore can safely conclude that the reaction of the α-hydroxy radical with MV^{2+} is indeed an electron transfer reaction with very little, if any, complications by other reactions.

Formation of $MV^{+\cdot}$ in the Presence of Au/PVA Solutions. The addition of the Au/PVA catalyst to the solutions described above may interfere in the sequence of reactions leading otherwise to the formation of $MV^{+\cdot}$. This possibility was investigated in deaerated solutions of 10^{-4} M MV^{2+} containing 1% 2-propanol, 1% acetone, and PVA or the Au/PVA catalyst. No effect on the yield of absorbance at 605 nm or the rate of its formation was observed, as indicated in some representative results shown in Table I. We conclude therefore that no interference of the Au/PVA system in the formation of $MV^{+\cdot}$ occurs under the experimental conditions used. This observation,

TABLE I: Yield and Rates for the Formation of $MV^{+\cdot}$ and Its Dimer in the Various Systems Studied[a]

additives	A_{605}[b]	A_{605}/A_{535}[b]	$10^{-5} \times k_5$,[c] s^{-1}	k_{605}/k_{535}[d]
	0.459	2.2	3.2	0.95
1.2×10^{-2} M PVA	0.494	2.3	3.5	1.0
2.7×10^{-4} M Au/1.2×10^{-2} M PVA	0.477	2.1	3.6	1.1
3.1×10^{-3} M PVS	0.269	1.16	2.0	1.8
5.2×10^{-4} M Au/6.0×10^{-3} M PVS	0.243	1.02	2.2	2.3

[a] Contain 10^{-4} M MV^{2+} in deaerated 1% acetone and 1% 2-propanol at pH 7. [b] Absorbance at the indicated wavelength at the end of its formation following a 10-ns pulse in 2-cm cells. [c] Pseudo-first-order rate constant obtained following the absorbance formation at 605 nm (reaction 5). [d] Ratio of the pseudo-first-order rate constants obtained following the absorbance at the two indicated wavelengths.

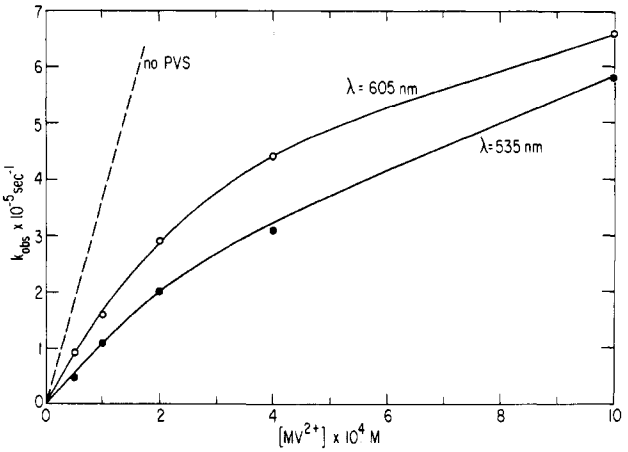

Figure 1. The dependence of the observed rate constant for the formation of the absorbance at 605 and 535 nm on $[MV^{2+}]$ at 6.2×10^{-3} M PVS and pH 7 following a 2-ns pulse.

however, is in clear contrast with the results in the Au/PVS system described below.

Formation of $MV^{+\cdot}$ and Its Dimer in Au/PVS Solutions. Changing the catalyst stabilizer from PVA to PVS causes a distinct change in the formation rate and yield of $MV^{+\cdot}$. These changes, however, are entirely attributable to the polyelectrolyte properties of PVS rather than to the catalyst as such. Because of the high potential field of the PVS polymer, condensation of MV^{2+} along this polymer is expected. The exclusion of negatively charged reactants from this field will strongly inhibit the reaction of e_{aq}^- with MV^{2+}.[14] This condensation will also reduce somewhat the rate of the reaction of uncharged reactants with MV^{2+} when this rate approaches the diffusion-controlled limit due to the inhibited diffusion of MV^{2+}. As can be seen in Table I, such is the case for the reaction of $(CH_3)_2\dot{C}OH$ radicals with MV^{2+} in the presence of PVS. It was verified that, when 2-propanol is omitted from the solution (the OH· radicals will then produce secondary radicals on the polymer), hardly any $MV^{+\cdot}$ radicals are produced from the polymer radicals. The dependence of the observed pseudo-first-order rate constant on $[MV^{2+}]$ at constant [PVS] is shown in Figure 1. The observed rate constant seems to level off at higher concentrations of MV^{2+}. A similar

(13) (a) Gordon, S.; Schmidt, K. H.; Hart, E. J. *J. Phys. Chem.* **1977**, *81*, 104. (b) Schmidt, K. H.; Gordon, S. *Rev. Sci. Instrum.* **1979**, *50*, 1656. (c) Meisel, D.; Schmidt, K. H.; Meyerstein, D. *Inorg. Chem.* **1979**, *18*, 971.

(14) Jonah, C. D.; Matheson, M. S.; Meisel, D. *J. Phys. Chem.* **1977**, *81*, 1805.

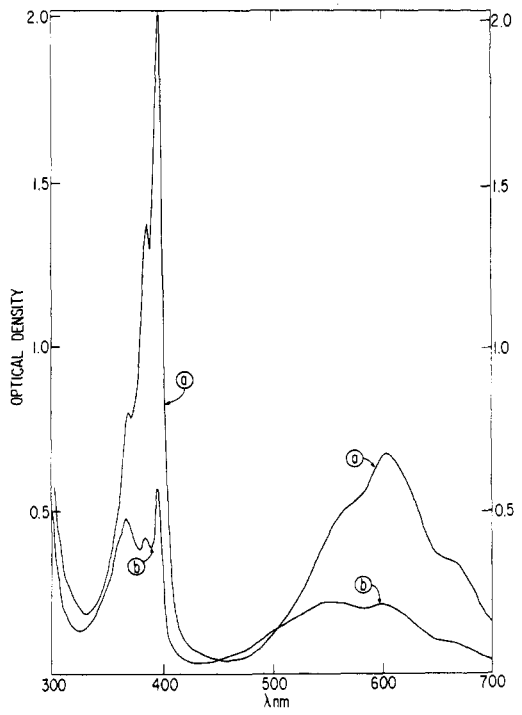

Figure 2. Spectra of $MV^{+\cdot}$ and its dimer following γ irradiation of 10^{-4} M MV^{2+}, 1% 2-propanol, and 1% acetone at pH 7: (a) no PVS; (b) 3.1×10^{-3} M PVS.

trend is observed at constant $[MV^{2+}]$ and varying [PVS]. Qualitatively this behavior may be explained by viewing the reaction as proceeding in two steps. First, $(CH_3)_2\dot{C}OH$ radicals diffuse toward the polymer with a rate independent of $[MV^{2+}]$. Second, these radicals react with MV^{2+} with a rate proportional to the number of MV^{2+} in the potential field of the polymer.

The most striking effect of PVS is on the product of the reaction of $(CH_3)_2\dot{C}OH$ with MV^{2+}. As is clear from the results in Table I or from the differences between the rate of formation of the absorbances at 605 and 535 nm (Figure 1), $MV^{+\cdot}$ is not the only product of this reaction when PVS is present. The spectra of these products following γ radiolysis of MV^{2+} solutions in the presence and the absence of PVS are shown in Figure 2. Spectra similar to the one shown in Figure 2b were obtained ca. 10 μs after a 20-ns linac pulse by using the streak camera technique. The close similarity between these spectra and the spectrum given by Kosower and Cotter[15] leads us to believe that these are attributable to the dimer of $MV^{+\cdot}$ (eq 7). Using

$$2MV^{+\cdot} \rightleftharpoons (MV^{+\cdot})_2 \qquad (7)$$

the extinction coefficients given by Kosower and Cotter for the dimer, we conclude that under the experimental conditions of Figure 2 most of the radical cation is converted to the dimer. This was found to be the case for most of the PVS-containing solutions ([PVS] = 0.6×10^{-3}–6×10^{-3} M at $[MV^{2+}] = 10^{-4}$ M and $[MV^{2+}] = 1 \times 10^{-4}$–$8 \times 10^{-4}$ M at [PVS] = 3×10^{-3} M). Since for the dimer $\epsilon_{535} = \epsilon_{605}$ (while $\epsilon_{605}/\epsilon_{535} = 2.2$ for the monomer), the ratio of the absorbances at these wavelengths should be unity when all $MV^{+\cdot}$ is converted to $(MV^{+\cdot})_2$. This was used as a convenient indicator of the amount of conversion in the PVS-containing solutions (cf. Table I). It should be noted that in the absence of PVS less than 1% conversion of $MV^{+\cdot}$ is to be expected from the association constants available in the literature[16] for similar viologen radicals (K_7 $\sim$ 500 M^{-1} at room temperature). The high extent of association observed in the PVS solutions is again an effect of the high potential field of the polymer. While $MV^{+\cdot}$ is expected to associate only to a small degree with the polymer field, $(MV^{+\cdot})_2$ would strongly condense along that field. The chemical potential thus established will divert practically all of the $MV^{+\cdot}$ initially produced into the dimeric form in the polymer field. Efforts to determine the kinetics of this conversion were defeated because of the lack of temporal separation between reactions 5 and 7 under a wide variety of conditions. It is clear however from Figure 1 and Table I that in PVS-containing solutions the rate of production of the absorption at 535 nm, where the contribution from the dimer dominates, lags behind the production of the absorption at 605 nm. Nonetheless, in no case were we able to actually observe the decay of $MV^{+\cdot}$ to $(MV^{+\cdot})_2$, in spite of the large ratio of $(\epsilon_{MV^{+\cdot}}/\epsilon_{(MV^{+\cdot})_2})_{605}$, due to the overlap in the rates of these two reactions.

TABLE II: Yield of H_2 from $MV^{+\cdot}$ in Au/PVA Solutions[a]

dose rate, krd/min	dose, krd	$[H_2]_0$,[b] μM	$[H_2]$,[c] μM	$G(H_2)/G(H_2)_0$
8.1	8.1	10.6	17.5	1.65
8.1	16.2	20.6	31.2	1.51
8.1	32.4	41.4	71.4	1.72
4.4	17.6	19.7	38.2	1.94
1.85	14.8	17.0	29.7	1.75
0.72	170.0	121.8	204.5	1.68
1.41	7.1	7.4	11.2	1.51
1.41	14.1	15.0	23.9	1.59
1.41	28.3	28.3	54.0	1.91
1.41	42.4	47.8	71.1	1.49
4.6	23.0	27.9	51.1 (4.3×10^{-5})	1.83
4.6	23.0	28.0	51.9 (1.1×10^{-4})	1.85
4.6	23.0	28.7	43.3 (5.4×10^{-4})	1.51
4.6	23.0	18.4	20.4, pH 7	1.11

[a] All solutions are Ar-saturated containing 1% v/v 2-propanol and acetone, 2×10^{-4} M MV^{2+} at pH 2.4 unless otherwise stated. [b] No Au but 1.1×10^{-2} M PVA. [c] In the presence of Au, the concentration of which is 2.7×10^{-4} M unless otherwise given in parentheses. [Au]/[PVA] = 2.4×10^{-2} constant.

Hydrogen Production in the Presence of Au Sols. The use of $MV^{+\cdot}$ as a source for molecular hydrogen has been demonstrated in a wide variety of chemical systems.[2-8] In particular, its use in photochemical energy conversion and

(15) Kosower, E. M.; Cotter, J. L. *J. Am. Chem. Soc.* **1964**, *86*, 5524.

(16) Evans, A. G.; Evans, J. C.; Baker, M. W. *J. Chem. Soc., Perkin Trans. 2* **1977**, 1787; *J. Am. Chem. Soc.* **1977**, *99*, 5882.

(17) Steckhan, E.; Kuwana, T. *Ber. Bunsenges. Phys. Chem.* **1974**, *78*, 253.

(18) Kuhn, A. T.; Byrne, M. *Electrochim. Acta* **1971**, *16*, 391.

(19) Bockris, J. O'M.; Reddy, A. K. N. "Modern Electrochemistry"; Plenum Press: New York, 1970; Vol. 2, p 1231.

(20) (a) Pentland, N.; Bockris, J. O'M.; Sheldon, E. *J. Electrochem. Soc.* **1957**, *104*, 182. (b) Conway, B. E. *Proc. R. Soc. London, Ser. A* **1960**, *256*, 128. (c) Bockris, J. O'M.; Parsons R. *Trans. Faraday Soc.* **1948**, *44*, 860.

(21) As might be expected, however, for Pt the rate of protonation and desorption are not the limiting rates, and only one decay process was observed.[11]

(22) (a) Turkevich, J.; Stevenson, P. C.; Hillier, J. *Discuss. Faraday Soc.* **1951**, *11*, 55. (b) Turkevich, J.; Garton, G.; Stevenson, P. C. *J. Colloid Sci., Suppl.* **1954**, *1*, 26.

(23) From ref 22. One might expect a radius of 100 Å for the particles. However, a radius of 40 Å for the gold particles is also in good agreement with the spectral features observed in our preparations and those expected from the Mie theory.[22b] Further, such a radius provides better agreement between the measured and calculated diffusion-controlled rate constants for MV^+ and (Au)$_n$ as well as between two gold particles.

(24) Wiegner, G.; Tuorila, P. *Kolloid—Z.* **1926**, *38*, 3.

storage systems is often discussed. In the present study we investigated the efficiency of the hydrogen production from water by $MV^{+}\cdot$ on gold catalysts (reaction 8). The

$$2MV^{+}\cdot + 2H_2O \xrightarrow{(Au)_c} 2MV^{2+} + H_2 + 2OH^- \quad (8)$$

radical cation (or its dimer) was produced by γ radiolysis of deaerated solutions containing 1% 2-propanol, 1% acetone, 2×10^{-4} M MV^{2+}, and the Au catalysts. Since reactions 1 and 4 produce hydrogen as well, blank solutions containing the same components (sols' stabilizers included) and at the same concentrations, except Au itself, were simultaneously irradiated with the Au-containing solutions. Both were then analyzed for H_2 by gas chromatography. Table II presents some results on H_2 yields in the Au/PVA system. It can be seen from Table II that the increased yield of H_2 in the Au/PVA solutions is independent of dose, dose rate, or concentration of gold sol. At pH 7, however, practically no increase in the yield of H_2 is obtained. The yield of H_2 in the absence of the catalyst is given by its yield from reactions 1 and 9 followed by reaction 4. This yield is therefore calculated with eq 10.

$$e_{aq}^- + H^+ \rightarrow H\cdot \quad (9)$$

$$G(H_2)_0 = G_{H_2} + G_H + G_{e_{aq}}\cdot k_9[H^+]/\{k_9[H^+] + k_2[(CH_3)_2CO]\} \quad (10)$$

Under the conditions of Table II (pH 2.37) this yields $G(H_2)_0 = 1.30$ molecules/100 eV. On the other hand, in the presence of the catalyst the maximum yield of H_2 is $G(H_2)_{max} = G(H_2)_0 + {}^1/_2G(MV^+) = 4.4$ molecules/100 eV. It is apparent from Table II that this maximum yield is not achieved under any of these conditions. It is also clear, from the previous section, that the reduced yield of H_2 is not a result of any disruption in the sequence of reactions that produces $MV^{+}\cdot$. The apparent low yield of catalyzed H_2 production should therefore be attributed to catalytic reactions, other than reaction 8, which do not produce hydrogen.[25] It was noted that no $MV^{+}\cdot$ absorption was present in the irradiated solutions at pH <7 at the end of the irradiation period (see also the next section). At higher pHs, however, a substantial amount of $MV^{+}\cdot$ was present in the Au-containing solutions for long periods of time.

One ready source for loss of reduction equivalents is through the reaction with the radiolytically produced H_2O_2 (eq 11). This would account for the loss of $2G_{H_2O_2} = 1.4$

$$2MV^{+}\cdot + H_2O_2 \xrightarrow{(Au)_c} 2MV^{2+} + 2OH^- \quad (11)$$

molecules/100 eV equivalents of $MV^{+}\cdot$. From the redox potentials for the couples involved ($E^\circ_{H_2O_2/H_2O} = 1.78$ V), reaction 11 is highly exoergic and is therefore possible. On the other hand, electron transfer from $MV^{+}\cdot$ to H_2O_2 will simply initiate a chain reaction in the absence of the catalyst. If no other reactions of $MV^{+}\cdot$ would occur (except reaction 11), one expects then, under the experimental conditions of Table II, $G(H_2)/G(H_2)_0 = 2.8$. The experimentally obtained average value of $G(H_2)/G(H_2)_0 = 1.7$ indicates that ca. 38% of $MV^{+}\cdot$ reacts in the hydrogen production reaction under these conditions. The nature of the competing reaction will be discussed in the succeeding section.

The lack of an appreciable amount of H_2 production from $MV^{+}\cdot$ at higher pHs is readily explained by the decrease in the reduction potential of the $H^+/{}^1/_2H_2$ couple. At such pHs ($E^\circ_7 = -0.41$ V for $H^+/{}^1/_2H_2$ and -0.45 V for $MV^{2+}/MV^{+}\cdot$)[17] the redox potentials of the two couples are too close to one another, and the overpotential that accumulates on the particles would not reach the one required for the hydrogen production reaction. A similar potential effect limits H_2 production in the Au/PVS system. The yield of hydrogen in Au/PVS solutions under conditions similar to those described in Table II for the Au/PVA system gave the ratio $G(H_2)/G(H_2)_0 = 1.1 \pm 0.1$ (conditions studied were in the following ranges: dose rate, 0.72–8.1 krd/min; doses, 17–70 krd; $[MV^{2+}] = 0.2$–10 mM; $[Au] = 0.7 \times 10^{-4}$–$5 \times 10^{-4}$ M; pH 2.1 and 7.0). As was shown in the previous section, a substantial fraction of $MV^{+}\cdot$ dimerizes in the presence of PVS. This dimerization would necessarily reduce the free energy available for reaction 8, and again the overpotential for the hydrogen production would not be attained. Nonetheless, no absorption in the spectral range where $MV^{+}\cdot$ and its dimer absorb could be observed at the end of the irradiation and at the lower pH in this system.

Kinetics of the Catalyzed Reactions of $MV^{+}\cdot$. The kinetics of the disappearance of $MV^{+}\cdot$ in the presence of the Au catalysts were studied by pulse radiolysis. In view of the problems of dimer formation and lack of H_2 production when PVS was used as the sol stabilizer, efforts were concentrated on the Au/PVA system. However, the disappearance of $MV^{+}\cdot$ and its dimer was clearly catalyzed in the Au/PVS system as well. Typical results are shown in Figure 3 for the Au/PVA system. The following qualitative observation can be pointed out before quantitative analysis is attempted. A fast decay of $MV^{+}\cdot$ is observed in the presence of Au/PVA in the few-millisecond range. (Note that $MV^{+}\cdot$ is stable for hours in the absence of the catalyst.) As can be seen in Figure 3a, this process leads to some bleaching of the absorbance of the original solution in the same spectral range where $MV^{+}\cdot$ also absorbs light. Since the only component of the original solution that absorbs light in this region is the Au sol, we have to conclude that this reaction involves both $MV^{+}\cdot$ and the Au/PVA sol. This bleaching persists for long periods of time, even on time scales longer than that of the slow process to be discussed later. The amount of $MV^{+}\cdot$ that reacts in this fast process is limited by the amount of Au catalyst available. Thus in Figure 3b we observe that, when the pulse width is increased to produce ca. 3 times higher $[MV^{+}\cdot]$ than in Figure 3a, some residual $MV^{+}\cdot$ absorption is left at the end of the fast process. On the other hand, when [Au] is increased, the fast process extends to larger amounts of $MV^{+}\cdot$ (compare Figure 3d with 3b). We conclude therefore that the fast process proceeds as long as there are sites available on the catalyst. Following this fast process a slower process is observed when $MV^{+}\cdot$ is further supplied to the system in which the Au catalyst was previously saturated (cf. Figure 3c).

The kinetics of the fast process were studied under a variety of conditions. The rate of the slow process increases with increasing acidity; therefore, to avoid overlap between the fast and the slow processes, we studied the former at a relatively high pH of 4.8. In Table III we summarize some of the effects studied. As can be seen in Table III, no effect of [PVA] or $[MV^{2+}]$ could be observed on the rate of the fast process in the initial stages of the reaction (first pulse of 2 ns). Furthermore, since increasing the concentration of MV^{2+} from 10^{-4} to 10^{-3} M did not affect the final level of absorbance at the end of the fast process (first 10-ns pulse), we conclude that MV^{2+} does not participate in an equilibrium that might have led to the

(25) Hydrogenation of MV^{2+} on colloidal Pt catalysts has been recently reported and products were analyzed: Johansen, O.; Lane, J. G.; Launikonis, A.; Mau, A. W. H.; Sasse, W. H. F.; Swift, J. D. Abstracts of the 3rd International Conference on the Photochemical Conversion and Storage of Solar Energy, Boulder, CO, 1980, p 145.

TABLE III: Kinetics of the Fast Decay of $MV^{+\cdot}$ in Au/PVA Solutions[a]

[Au], mM	[PVA], mM	$[MV^{2+}]$, mM	pulse width (ns)/pulse number[b]	A_0[c]	A_∞[c]	k_{obsd},[d] s^{-1}
0.17	5.5	0.2	2/1	0.087	−0.014	1.3×10^3
0.17	5.5	0.2	2/2	0.086	0.031	
0.17	5.5	0.2	2/3	0.086	0.060	
0.17	5.5	0.2	2/4	0.087	0.072	
0.17	5.5	0.2	10/1	0.240	0.082	
0.17	11.0	0.2	2/1	0.076	−0.019	1.2×10^3
0.33	11.0	0.2	2/1	0.075	−0.014	3.0×10^3
0.33	11.0	0.2	2/5	0.070	0.012	
0.33	11.0	0.2	10/1	0.263	−0.052	
0.17	5.5	0.1	2/1	0.078	−0.017	1.4×10^3
0.17	5.5	0.1	10/1	0.240	0.074	
0.17	5.5	1.0	2/1	0.080	−0.012	1.6×10^3
0.17	5.5	1.0	10/1	0.260	0.085	

[a] All experiments at pH 4.8 ± 0.1 in deaerated solutions containing 1% 2-propanol and 1% acetone. [b] Pulse width in nanoseconds followed by the pulse number in repetitive pulsing. [c] A_0 and A_∞ are initial and final absorbances, respectively, for the fast process in 1-cm cell. [d] Pseudo-first-order rate constant for the decay of $MV^{+\cdot}$ ± 15%.

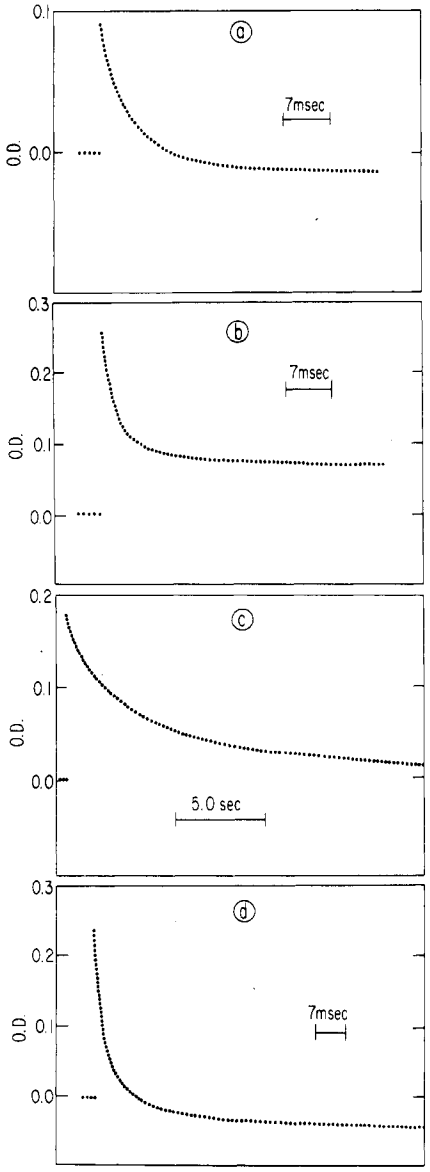

Figure 3. Decay of $MV^{+\cdot}$ in the presence of Au/PVA catalyst: (a) fast decay following first 2-ns pulse; $[MV^{2+}] = 2 \times 10^{-4}$ M, [Au] = 1.76×10^{-4} M, [PVA] = 5.5×10^{-3} M; 1% 2-propanol and 1% acetone; pH 4.8; (b) fast decay following first 10-ns pulse; same conditions as in a; (c) slow decay following second 10-ns pulse; same conditions as above; (d) fast decay following first 10-ns pulse; same conditions as above except [Au] and [PVA] doubled.

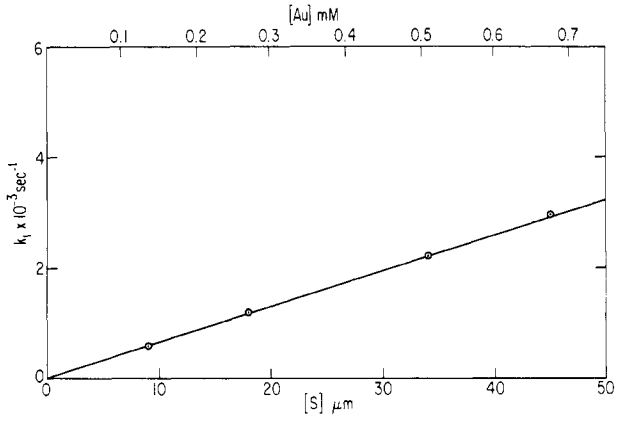

Figure 4. The dependence of the fast decay process of $MV^{+\cdot}$ on [Au]. $[MV^{2+}] = 2 \times 10^{-4}$ M; pH 4.0 ± 0.1; [Au]/[PVA] = 2.8×10^{-2}. All other conditions as in Figure 3. Upper scale: initial [Au]. Lower scale: concentration of sites.

saturation effect observed under these conditions. When the acidity was increased to 10^{-2} M $HClO_4$, hardly any effect on k_{obsd} of the fast process was observed. Neither could we observe any change in the level at which saturation was obtained at these high acidities. We therefore conclude that the saturation level is not determined by consumption of H^+ (this is further corroborated by the results of the conductivity technique). We further conclude that, at least up to pH 4.8, a protonation reaction is not a rate-determining step in the mechanism leading to the decay of $MV^{+\cdot}$ in the fast process.

Increasing the ionic strength in the range of 3–30 mM shows a decrease in the rate of the fast decay from $k_{obsd} = 1.3 \times 10^3$ s^{-1} to 8.1×10^2 s^{-1} at 30 mM $NaClO_4$ (0.17 mM Au and 0.2 mM MV^{2+}). As would be expected for these hydrophobic sols, they seem to carry net negative charges. If one uses the Brønsted–Bjerrum equation $\log k/k_0 = 1.02 Z_A Z_B \mu^{1/2}/(1 + 0.329 r\mu^{1/2})$ and assumes that $Z_A = +1$ for $MV^{+\cdot}$ and $r = 40$ Å for the colloidal particle (see below), the primary salt effect indicates $Z_B = 8 \pm 1$. Such a charge on a conducting sphere of 40-Å radius in water (dielectric constant = 80) gives a potential of ~35 mV.

The rate of the fast process can be seen in Table III to increase on increasing [Au]. This rate constant was measured during the initial decay of $MV^{+\cdot}$ at the smallest pulse available (2 ns) where pseudo-first-order kinetics are applicable. As can be seen in Figure 4, the decay rate constant for this process increases linearly with [Au]. Under these conditions, sites that are already occupied by

$MV^{+\cdot}$ during the course of the reaction do not affect appreciably the reactivity of the remainder of the sites.

Assuming a spherical shape of 80-Å diameter for the gold particles, we can calculate the concentration of particles [P] from the density (19.3 g/cm^3), atomic weight, and initial concentration of gold. Such a calculation then yields [P] = [Au]/1.6 × 10^4. The slope of Figure 4 (4.4 × 10^6 M^{-1} s^{-1}, in terms of Au atoms) then yields 7.0 × 10^{10} M^{-1} s^{-1} in terms of gold particles. This experimentally obtained rate constant is in fact very close to the diffusion-controlled rate constant calculated from the Debye equation for particles of this size. (We should note that there is some uncertainty in our estimate of the size of the particles.[22,23]) The fast process observed is thus controlled by diffusion of $MV^{+\cdot}$ radicals to the Au particles. It is interesting to note that very similar rates were observed for the decay of $MV^{+\cdot}$ on Pt/PVA catalysts of the same particle size at concentrations similar to those used here.[11]

The results presented above can be rationalized on the basis of the mechanism suggested to operate in the catalysis of hydrogen production by reducing intermediates. The conceptual framework for this mechanism was suggested by Henglein[9] to be identical with the mechanism of the hydrogen evolution reaction on silver electrodes and was confirmed to operate also on gold sols.[12] The steps to be considered for the fast process will therefore include reactions 12–14. The rate constant calculated above is

$$MV^{+\cdot} + (Au)_c \rightleftharpoons (Au)_cMV^{+} \quad (12)$$

$$(Au)_cMV^{+} \rightleftharpoons (Au)_c^{-} + MV^{2+} \quad (13)$$

$$(Au)_c^{-} + H_2O \text{ or } H_3O^{+} \rightleftharpoons (Au)_cH + OH^{-} \text{ or } H_2O \quad (14)$$

k_{12} in this scheme of reactions. Reactions 12–14 through repetition lead to a multicharged particle with adsorbed radicals ($MV^{+\cdot}$ and H), and thus the gold particle acts as a microelectrode.

Since the value of the rate constant for the fast decay process indicates a diffusion-controlled reaction, one may conclude that every encounter of $MV^{+\cdot}$ with the particles surface is fruitful in initiating the sequence of reactions 12–14. This may in turn lead to the conclusion that the entire surface of the particle effectively serves as active sites for $MV^{+\cdot}$. We therefore shall now proceed to determine the number of effective sites on the particles.

Determination of the Effective Number of "Sites". As was shown in the previous section, the reaction of $MV^{+\cdot}$ proceeds until saturation of the surface of the particles is attained. From the results such as those in Figure 3b, the concentration of effective sites can therefore be estimated. It has, however, to be emphasized that the term "sites" is used here in the broadest meaning and will simultaneously include the amount of charge that a particle can accommodate as well as actual binding sites. For this determination the dependence of the initial and final absorbances, A_0 and A_∞, respectively, were measured as a function of the dose delivered by the electron pulses and the initial concentration of gold. In Table IV we present some results of such studies. Since changes are observed in the absorption spectra of the original solution upon adsorption, the first step would be to determine an effective $\Delta\epsilon_S$ (at 605 nm) which represents the difference in the extinction coefficient of a site before and after adsorption of the products in reactions 12–14. This was calculated from the results where bleaching of the original solutions was observed (such as in Figure 3a) and where it was clear that the total available sites have not been occupied (i.e., on further injection of $MV^{+\cdot}$ by a bigger pulse still more radicals could decay by the fast process).

TABLE IV: Determination of the Concentration of Active Sites and the Effective Extinction Coefficient of Au/PVA Sol[a]

[Au], mM	$[MV^{+\cdot}]_0$,[b] μM	A_0	A_∞[c]	$10^{-3} \times \Delta\epsilon_{site}$,[d] M^{-1} cm^{-1}	[S],[e] μM
0.055	7.0	0.083	0.028		3.6
0.055	13.6	0.160	0.105		3.6
0.137	7.4	0.087	−0.025	3.38	
0.137	14.4	0.170	0.024		9.6
0.137	23.8	0.281	0.140		9.2
0.273	7.4	0.087	−0.021	2.84	
0.273	14.4	0.170	−0.050	3.47	
0.273	22.2	0.262	0.000		17.0
0.273	48.7	0.575	0.340		15.0
0.273	75.3	0.889	0.690		13.0
0.520	8.0	0.094	−0.025	3.12	
0.520	13.8	0.163	−0.060	4.35	
0.520	23.7	0.280	−0.085	3.59	
0.520	50.8	0.600	0.020		38.0
0.520	75.0	0.885	0.330		36.0

[a] In deaerated solutions containing 2 × 10^{-4} M MV^{2+} at pH 4.0 ± 0.1, [Au]/[PVA] = 2.8 × 10^{-2} constant. Optical path of 1 cm; all measurements at λ = 605 nm. [b] Initial concentration of $MV^{+\cdot}$ produced by the pulse. Assuming ϵ_{605} = 1.18 × 10^4 M^{-1} cm^{-1} for $MV^{+\cdot}$. [c] Negative sign signifies bleaching of original absorption. [d] Extinction coefficients difference between an empty and an occupied site. [e] Concentration of active sites.

This $\Delta\epsilon$ was then calculated from $\Delta\epsilon_S = A_\infty/[MV^{+\cdot}]_0$ and is given in Table IV. Implicit in this calculation is the assumption that equilibrium 12 is strongly shifted toward the products. Since no effect of $[MV^{2+}]$ on A_∞ was observed and since the obtained $\Delta\epsilon_S$ is reasonably constant, this assumption is correct within our experimental error. The average value obtained, $\Delta\epsilon_S$ = 3.5 × 10^3 M^{-1} cm^{-1} (per mole of sites), may be compared to ϵ_{605} = 2.0 × 10^3 M^{-1} cm^{-1} (per total g atom) obtained from the linear dependence of the absorption of the original sol on [Au] before irradiation. We can now proceed to calculate the concentration of available sites on the surface.

Assuming again, and on the same grounds, that reaction 12 is shifted to the right, one calculates the concentration of available sites [S] from the experimental results where saturation of the particles is observed (cf. Table IV). This quantity was calculated by using $[S] = [MV^{+\cdot}]_0 - [MV^{+\cdot}]_\infty$ where $[MV^{+\cdot}]_\infty$ is the concentration of free $MV^{+\cdot}$ at the end of the fast process. The latter is calculated from

$$[MV^{+\cdot}]_\infty = \frac{A_\infty + \Delta\epsilon_S[MV^{+\cdot}]_0}{\epsilon_{MV^{+\cdot}} + \Delta\epsilon_S}$$

In Figure 5 we present the dependence of [S] on initial [Au]. From the slope of this figure, one estimates that 6.6% of the total amount of gold atoms can serve as active sites. The conductivity experiments (see below) indicate that reaction 11 occurs during this stage. Since $2G_{H_2O_2} = 0.22G(MV^{+\cdot})$, this would mean that we have overestimated the number of active sites by 22%. We conclude therefore that 5.1% is a more realistic estimate. On the other hand, the percentage of the surface atoms out of the total number of atoms can be estimated from the radius of the particles (r_p = 40 Å) and the atomic radius of gold (r_A = 1.4 Å) to be $[r_P^3 - (r_P - 2r_A)^3]/r_P^3$ = 19%. One concludes that ca. four surface gold atoms can serve as an active site for each $MV^{+\cdot}$.[23] The roughness and imperfections of the surface are probably major contributions to this high efficiency of the surface. We can also reconstruct the spectrum of the products of reactions 12–14. This was done by measuring the spectrum of the products at the end of the fast process by using the streak camera technique. As-

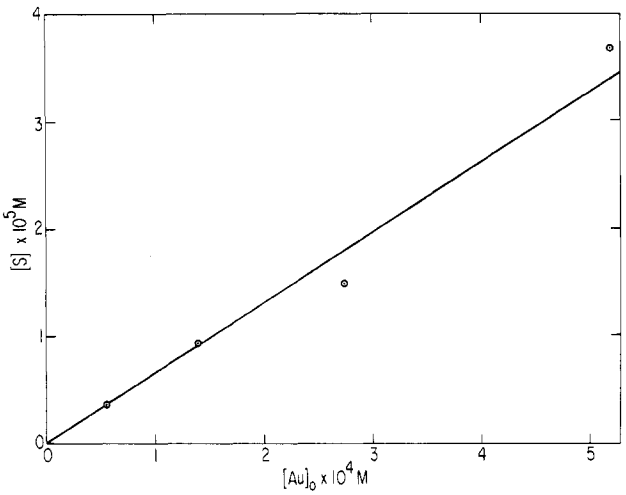

Figure 5. Concentration of available sites as a function of initial concentration of gold; experimental conditions as in Table IV.

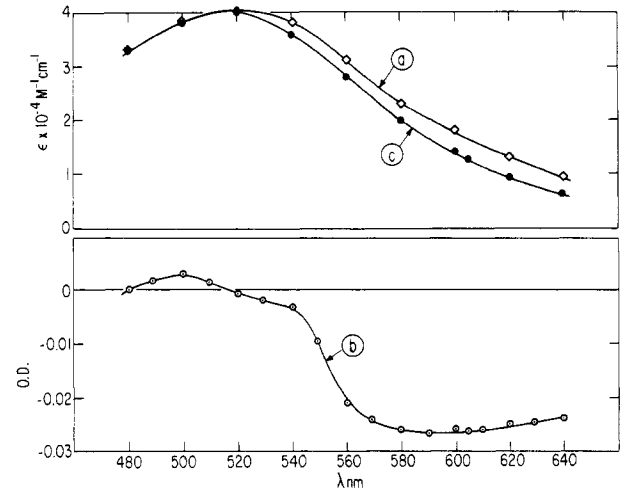

Figure 6. Spectrum of the Au/PVA sol: (a) before irradiation; (b) difference spectrum at the end of the fast decay process; obtained by using the streak camera technique following a 4-ns pulse on a solution containing 2 × 10^{-4} M MV^{2+} and 3.0 × 10^{-4} M Au/1.1 × 10^{-2} M PVA at pH 4.5; (c) calculated spectrum of the products; ε is given in terms of concentration of sites for both a and c; optical path, 1 cm.

suming that each $MV^{+\cdot}$ produces either of the products of reactions 12–14, we show the calculated spectrum of these products in Figure 6c. Also shown in Figure 6 are the difference spectrum (Figure 6b) and the spectrum of the original solution (Figure 6a). It seems therefore from Figure 6 that the spectrum of the sol plus adsorbed radicals (MV^+, H or e^-) is rather similar to the original sol spectrum except for some narrowing of the width and a slight blue shift.

Products of the Fast Processes. We now turn to the question of the various possible products of the fast process. The possibilities to be considered are adsorbed $MV^{+\cdot}$ radicals (reaction 12), accumulated charges (reaction 13), adsorbed H· atoms (reaction 14), or any combination of these. It can be shown that unbalanced charges (e^- or $MV^{+\cdot}$) cannot constitute a large fraction of the "sites" on the level of [S] found in the previous section. Any substantial fraction of [S] that would stay as free charges would create an unreasonably high potential on the surface of the particles. On the other hand, the salt-effect studies described above indicate a rather small net charge on the particle at pH 4.8. Seeking to elucidate the identity of the occupied sites, we found that saturation of solutions with H_2 suppressed a large portion of the fast reaction of $MV^{+\cdot}$

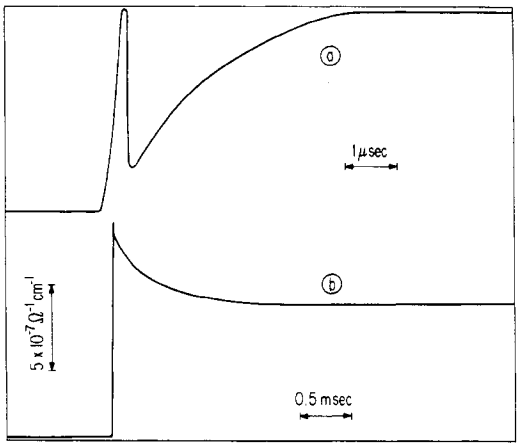

Figure 7. Conductivity changes on the formation (a) and the catalyzed disappearance (b) of $MV^{+\cdot}$ in Au/PVA sols; experimental conditions as in Figure 3; pulse width, 0.2 μs; total dose, 0.95 krd.

without affecting the slow process. Surface adsorption of H_2 is not likely to be the source of this effect, however, since reaction 15 has been shown to be very slow on gold

$$H_2 + (Au)_c\cdot \rightleftharpoons (Au)_cH \qquad (15)$$

sols.[12] Experiments with D_2 or H_2/D_2 mixtures showed very little HD formation in 2 h at pH 5–1.3 and in the presence of MV^{2+} on gold sols, confirming that reaction 15 is slow even in acid solutions.

The amount of protonation occurring in the fast process was studied by using the pulse radiolysis–conductivity technique. In Figure 7, we show typical conductivity signals obtained on pulse irradiating solutions similar to those on which the spectrophotometric results of Figure 3 were obtained. The main contribution to the conductivity signals is from changes in $[H^+]$. Following the fast formation and decay of H^+ (reactions 1 and 2), a slower increase in the conductivity signal is observed due to reaction 5 (Figure 7a). This signal then decays at a rate similar to the decay rate of $MV^{+\cdot}$ in the fast process as discussed above. However, as can be seen in Figure 7b, only ca. 30% of the H^+ which is produced by reaction 5 actually disappears at this stage of the catalysis under the experimental conditions of Figure 7. Further, since reaction 11 has to be considered in this system, its occurrence during this stage would account for most of the H^+ consumed in the fast process. At any rate, it seems that most of the $MV^{+\cdot}$ radicals are adsorbed on the particle (reactions 12 and 13) with equilibrium 13 slightly shifted to the right. However, only a small percentage, if any, is proceeding along reaction 14 during the fast reaction.

Decay of $MV^{+\cdot}$ in the Slow Process. Product Desorption. Analysis of the decay kinetics in the slow process is even more complicated since no single final product is obtained in these systems. Nevertheless, the effects of [Au], $[H^+]$ and $[MV^{+\cdot}]$ on the decay kinetics of $MV^{+\cdot}$ in the slow process were studied. At pH ≤2, the decay of $MV^{+\cdot}$ seems to follow a pseudo-first-order rate law while at higher pH the decay rate did not fit clean first- or second-order kinetics. The effect of $[H^+]$ at the lower pH range is shown in Table V. In this pH range, the observed rate constant was linearly dependent on $[H^+]$. At the higher pHs the dependence on $[H^+]$ was even more pronounced. However, because of the undefined rate law in this region (2 < pH < 4.5), quantitative analysis was not attempted. Also shown in Table V is the effect of dose on the observed rate. Although the decay rate could be fitted reasonably well to a first-order rate law, we believe that the reaction is closer to zero order in $MV^{+\cdot}$. As can be seen

TABLE V: Effect of Acidity and Dose on Rate of Decay of $MV^{+\cdot}$ in the Slow Process[a]

[H⁺], M	pulse width (ns)/pulse number[b]	$[MV^{+\cdot}]_{slow}$,[c] μM	$\tau_{1/2}$, ms	10^2(initial rate), M/s
1×10^{-2}	10/1	7.7	29.7	179.4
	10/2	26.1	69.3	184.0
	20/1	30.4	73.0	288.0
	40/1	54.1	121.6	308.4
2.6×10^{-2}	10/1	8.2	15.4	369.0
	10/2	26.5	28.2	450.0
	20/1	32.7	33.5	676.9
0.1	10/1	8.4	8.0	730.0
	10/2	32.1	12.9	1270.3
	20/1	31.5	13.9	1565.6
0.2	10/1	12.8	5.3	1676.8
	10/2	36.0	8.0	2018.4
	20/1	34.3	9.4	2538.2
1×10^{-2}, H_2-saturated	10/1	20.1	55.0	253.3
	10/2	42.3	79.7	193.1
	20/1	46.5	126.0	255.7
	40/1	69.7	192.5	250.9

[a] All contain 2×10^{-4} M MV^{2+} and 1.5×10^{-4} M Au/5.7×10^{-3} M PVA, Ar saturated, unless otherwise indicated. [b] Pulse width in nanoseconds followed by pulse number on consecutive pulsing. [c] Total amount of $MV^{+\cdot}$ reacted in the slow process.

in Table V, the decay rate is only slightly dependent on $[MV^{+\cdot}]$. This suggests that the rate-determining step does not involve $MV^{+\cdot}$. Rather, desorption processes (e.g., reaction 16) control the kinetics at this stage. It was, however, also noted that the rate of $MV^{+\cdot}$ disappearance decreased on consecutive pulsing after a large number of pulses. Apparently, a product of the catalyzed reaction which poisons the catalyst accumulates in these solutions. Since saturation of the solution with H_2 had little effect on the decay rate of $MV^{+\cdot}$ in the slow process, the poisoning product is not H_2.

The strong dependence of the rate of this process on $[H^+]$ may be explained by reactions 14 and 16 participating

$$(Au)_c^{n-}H_m + H_3O^+ \rightarrow (Au)_c^{(n-1)-}H_{m-1} + H_2 + H_2O \quad (16)$$

in the rate-determining step. It seems from the discussion in the previous section that the particles in reaction 16 also contain a large coverage by $MV^{+\cdot}$. Once sites are available, the sequence of reactions 12–14 is repeated. However, in view of the incomplete conversion of $MV^{+\cdot}$ to H_2, a parallel pathway for destruction of $MV^{+\cdot}$ has to exist (reaction 17).

$$MV^{+\cdot} + (Au)_c^{n-}H_m \rightarrow (Au)_c^{n-}H_{m-1} + (P) \quad (17)$$

Although the identity of the product in this reaction remains unresolved, one may speculate on its nature. It is rather unlikely that this product is the one electron reduction product of $MV^{+\cdot}$ in view of the low reduction potential of $MV^{+\cdot}$ (−0.77 V at pH 7[17]). More likely, hydrogenation of one of the pyridine rings is the side reaction.[25]

It was shown that on gold electrodes[18] at pH >0 coverage by adsorbed hydrogen atoms is very small. Under these conditions and at high current densities, the electrochemical desorption step (reaction 16) becomes the rate-determining step.[18,19] Consideration of the hydrogen atom recombination reaction on the surface of the particle as the rate-determining step is therefore unnecessary here. A similar conclusion was previously reached for the hydrogen evolution reaction on gold sols,[12] and, as will be shown below, the gold particles operate under conditions equivalent to high current densities. At pH <2 equilibrium

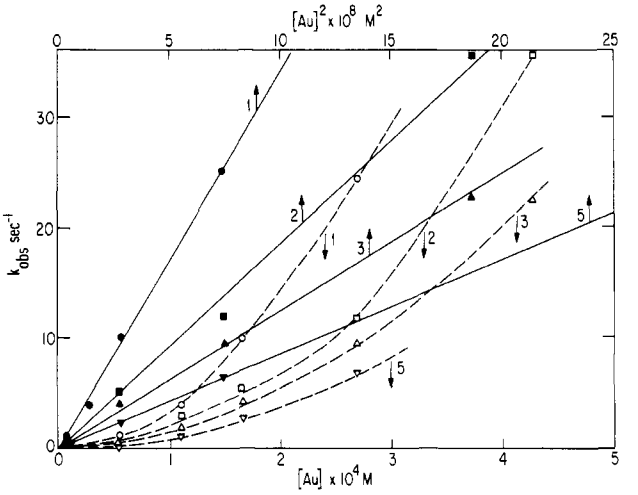

Figure 8. The dependence of the observed rate constant for the decay of $MV^{+\cdot}$ in the slow processes on [Au]. $[MV^{2+}] = 2 \times 10^{-4}$ M; pH 2.1. Dashed lines: lower scale. Solid lines: upper scale. Numbers refer to pulse number in consecutive pulsing; all are 10-ns pulses.

14 is rapidly attained as well as the maximum (and probably small) coverage by hydrogen atoms. Reaction 16 then becomes the only rate-determining step, and the rate of the reaction is first order in $[H^+]$, as is experimentally observed. Under such conditions, we obtain, from the dependence of the half-life on $[H^+]$ (Table V), $k_{16} = 740$ M^{-1} s^{-1} before an appreciable poisoning of the surface occurs. This rate constant however contains the dependence on [Au] and should be regarded only as pseudo-constant under the particular conditions of Table V.

The dependence of the observed rate of decay of $MV^{+\cdot}$ in the slow process on [Au] was measured at pH 2.1. As can be seen in Figure 8, the rate is strongly dependent on [Au] and seems to be of second order in [Au]. Since the adsorption stage is much faster than the rate of the slow process, one would expect the slow process to be of order 0–1 in [Au]. Nevertheless, in the case of the gold sols and, as was previously reported, in the case of Pt/PVA,[11] the rate of $MV^{+\cdot}$ decay is of order >1 in the concentration of the metal.[21] A possible explanation of this dependence on [Au] is that the rate-controlling step involves collisions between two gold particles (eq 18). The rate constant for

$$(Au)_c^{n-}-H_m + (Au)_c^{n-}-H_m \rightarrow 2(Au)_c^{n-}-H_{m-1} + H_2 \quad (18)$$

collisions between gold particles is 4.1×10^9 M^{-1} s^{-1} (independent of the size of the particles in the range of diameters 29–970 Å) according to Wiegner and Tuorila.[24] This rate constant was obtained from rates of coagulation of the particles and applied therefore to the uncharged particles. In the case under consideration, at the relatively high ionic strength ($\mu = 0.013$) and with the Debye equation, it can be shown that the electrostatic stabilization of the colloid is minimal. The rate constant for such collisions under the experimental conditions of Figure 8 is therefore close to that determined by Wiegner and Tuorila. Indeed, this rate constant combined with 6.25×10^{-9} M Au particles concentration yields a half-life of 0.027 s, in good agreement with Figure 8, where the half-life is ~0.028 s for the same gold concentration. Note that as shown earlier the 40-A° radius also gives an excellent agreement between the calculated and measured rate constants for the adsorption reaction of $MV^{+\cdot}$ on Au particles.

Two possibilities for reaction 18 as the rate-controlling step may be suggested. One is a hydrogen atom (or electron) transfer reaction between two particles to yield H_2

(or P) as depicted in reaction 18. A second possibility is that in a collision the massive Au particle perturbs the particle surface (or the adsorbed PVA molecules), perhaps ensuring H migration to give H_2. This biparticle reaction would be in competition with reaction 16 and would therefore be most efficient at pHs where reaction 14 is already shifted to the right while reactions 16 and 17 are still of comparable rate. This will also explain the mixed order observed in the decay of $MV^{+\cdot}$ at $4 > pH > 2$. At higher acidities and lower [Au] the contribution from the particle–particle reaction is rather small. The occurrence of this reaction in preference to chemical desorption of H_2 from a single particle would mean that migration of adsorbed H atoms is slow compared to the rate of the particle–particle reaction. Polarization in the metal induced by the approaching particle may also reduce the H–metal bond energy and facilitate H_2 desorption. However, the increased rate of the interparticle reaction will enhance the danger of coagulation of the sol.

A quantitative comparison with the hydrogen evolution reaction on gold cathodes may be of some interest. From the rate of decay of $MV^{+\cdot}$ in the slow process, one may estimate the current density flowing through the particles during the whole process from $MV^{+\cdot}$ to H_2 (or P). Under conditions of steady supply of radical, such as steady-state irradiation, the rate-limiting step is clearly not the rate of adsorption. Thus, for example, at 0.1 M H^+ and low $[MV^{+\cdot}]_0 = 8.4\ \mu M$ (Table V), i.e., when the surface is still clean of the poisoning product, the half-life for $MV^{+\cdot}$ is 8 ms at 1.5×10^{-4} M Au. This would mean an average of 5.6×10^4 of $MV^{+\cdot}$ ions are consumed at the surface of a single particle in 1 s (same assumptions as in the previous sections on the size of a particle). Since the surface area of the particles is 2.01×10^{-12} cm^2, the current density can be calculated to be 0.0045 A/cm^2. The highest current density however would be determined by the rate of the fast diffusion-controlled rate as discussed above. Although studies at very high acidities were avoided (primarily because of instability of the colloid), conditions where the mass transport of $MV^{+\cdot}$ to the particles would become the rate-determining step should be achievable. Thus at 1 M H^+ and 1.5×10^{-4} M Au, the extrapolated observed rate constant on a relatively clean surface would be $\sim 750\ s^{-1}$, which is somewhat smaller than the rate constant for the fast process at that ionic strength under the same experimental conditions. Under such conditions, the maximum possible current density would be $\sim 0.04\ A/cm^2$. At 0.1 M HCl current densities of $10^{-2}\ A/cm^2$ are obtained on gold cathodes at overpotentials of 0.4 V,[20a,b] while the maximum current density calculated above would correspond to 0.18 V at 1 N HCl.[20c] It is commonly accepted that under such high current densities the electrochemical desorption step is the rate-determining step[19] on gold electrodes, and all of the indications point to an equivalent step in the gold sols.

Finally, it should be noted that, at the end of the slow process, the particle is still not regenerated to its initial state. This can be seen from the persistence of the bleached absorbance at the end of the slow decay of $MV^{+\cdot}$ (cf. Figure 3). Part of this is probably due to the adsorbed poisoning product. However, since the particle is still active in the hydrogen production reaction, part of this persistent bleaching is due to radicals (MV^+, H or e^-) which are still adsorbed on the surface for long periods of time. Only on a much slower time scale could the recovery of this absorbance be observed. However, because of the smallness of this bleached absorbance and instability of the analytical light source on the time scale of minutes, a systematic study of this desorption was impractical.

Conclusions

To summarize this research, the following points are of particular interest.

(1) The stabilizer of the sol may in some cases play a decisive role in the hydrogen evolution reaction. Even when a seemingly inert stabilizer is used, electrostatic interactions may divert the reaction toward an undesired side reaction or even prevent the desired reaction. Thus, in the case of PVS as stabilizer, dimerization of the $MV^{+\cdot}$ radical in the potential field of the polymer dominates its further reactions.

(2) The rate of adsorption step is found to be controlled by diffusion. At practical pHs and catalyst concentrations, this step is not the rate-determining step. Protonation and desorption of products are the rate-determining steps. At $pH < 2$ desorption equivalent to that found in the electrochemical reaction dominates the rate. However, the possibility of an interparticle reaction is indicated even at pH close to 2.

Acknowledgment. Many discussions with Professor K. K. Kopple and the help of Dr. K. H. Schmidt with the conductivity experiments are much appreciated. The dedicated operation of the linac by Don Ficht and Lee Rawson and the assistance of Patricia Walsh and Robert Clarke are gratefully acknowledged.